ISSN 1330-3651(Print), ISSN 1848-6339 (Online)
UDC/UDK 629.783:528.93

WORLDVIEW-1 SATELLITE IMAGE PROCESSING FOR TOPOGRAPHIC MAPS CONTENT UPDATE

Goran Ćirović, Miodrag Regodić, Dragoljub Sekulović, Vladan Tadić, Ljubomir Gigović

Original scientific paper
Due to the possibilities it provides, remote sensing is the basic method for the creation and updating of maps, in our country and abroad. The use of satellite images in the development of cartographic products will have an increasingly important role in the future. Satellite missions that are engaged in the sale and distribution of satellite imagery have also become engaged in the processing of those images, which allows them to appear on the market not only with images, but with final data in widely-used public formats and coordinate systems. This work presents several digital processing methods used in the processing of satellite images, with special emphasis on orthorectification and georeferencing procedures, performed experimentally on high-quality WorldView-1 imagery.

Keywords: *processing, topographic maps, update, WorldView satellite image*

Obrada satelitskog snimka WorldView-1 za dopunu sadržaja topografskih karata

Izvorni znanstveni članak
Daljinska detekcija, zahvaljujući mogućnostima koje pruža, predstavlja osnovnu metodu izrade i ažuriranja karata u svijetu i kod nas. Primjena satelitskih snimaka će u budućnosti imati sve veću i značajniju ulogu u izradi svih kartografskih proizvoda. Satelitske misije koje provode prodaju i distribuciju snimaka obavljaju sve veći stupanj njihove obrade i na tržištu se pojavljuju ne samo sa snimcima već i s gotovim podacima u nekom od javnih formata i u nekom od široko rasprostranjenih koordinatnih sustava.U radu su u procesu obrade satelitskih snimaka predstavljeni neki postupci obrade digitalnih satelitskih snimaka, s posebnim osvrtom na postupke ortorektifikacije i georeferenciranja, što je eksperimentalno izvedeno na visoko kvalitetnom snimku WorldView-1.

Ključne riječi: *ažuriranje, obrada, topografske karte, WorldView satelitski snimak*

1 Introduction

Remote sensing images produced on platforms such as artificial Earth satellites, and the data they carry, have so far been exploited for military (reconnaissance) purposes and in various fields like meteorology, geology, agriculture, forestry, hydrology, and for some specific purposes, such as monitoring and prediction of natural phenomena, environmental protection and other [1, 2, 3].

Constant improvement of techniques and technology of satellite sensor systems enabled the commercial satellite companies (e.g. Space Imaging and DigitalGlobe) to take satellite images from space with spatial resolution from 0,4 to 1,0 m. The advent of satellite images of high spatial resolution – HRSI (IKONOS, QuickBird, WorldView and GeoEye) enabled the use of these digital images in the production of large scale digital geodetic layers and digital terrain models [4, 5, 6, 7, 8, 9]. In addition to their use in the preparation of topographic maps (TM) and survey plans, they are increasingly used in civil engineering industry during the design and construction planning, as well as monitoring of project implementation.

Imagery that is the subject of this paper is one of the newer products by the DigitalGlobe Company, delivered as a panchromatic satellite imagery of a wider Belgrade area made on the WorldView-1 satellite mission. The image was delivered in digital form, and pertains to the Basic satellite imagery group, which means that preprocessing performed includes radiometric correction and sensor correction, georeferencing in UTM WGS 84 projection without the use of control points. In order to be able to use this imagery for purposes of surveying, mapping, civil engineering and other application areas that require reliability and accuracy of measuring surface, it was necessary to carry out additional processing.

2 WorldView-1 satellite image processing

The experiment was carried out in May 2012 at the Military Geographical Institute (MGI) in Belgrade. The chosen test area was the southern part of Belgrade spreading over two sheets of topographic maps (429-2-4 and 429-4-2), scale 1:2500 (TM25), stretching from Ada Ciganlija in the north to urban neighbourhoods of Vidikovac, Rakovica and Bele Vode in the south. The eastern border is Kosutnjak hill, and the western boundary is Makis field and highway in the direction of Obrenovac (Fig. 1). The test area included the peripheral parts of the city, which contain areas with most additions since the last map update. Also, this area contains various types of surfaces in terms of hydrology, vegetation, and topography. The western part of the test area consists of plains with agricultural land; the central part consists of urban areas of the city of Belgrade, while Kosutnjak forest with elevations is predominant in the eastern part of the test area.

The experiment involved the processing of the image, which entailed orthorectification i.e. internal geometric correction and georeferencing i.e. external geometric transformation. The image processed in this manner is fully usable in further stages of production or update of geodetic survey maps. The experiment was carried out using the PCI Geomantic 9.1, ER Mapper 6.1 and ArcGIS 9.3 software.

2.1 Worldview-1 image characteristics

The imagery was delivered in digital form, and pertains to the Basic satellite imagery group, which means that pre-processing performed includes radiometric correction and sensor correction, georeferencing in UTM WGS 84 projection without the use of control points (Fig. 1).

Figure 1 The layout of the test area on the TM 25 and on the WorldView-1 satellite imagery

More detailed information on the WorldView-1 imagery is contained in the accompanying text file that was obtained along with the image. The most important data are extracted and shown in Tab. 1.

Table 1 WorldView-1 image data

Satellite mission	WorldView-1
Company	DigitalGlobe
Recording date	14. July 2011.
Earth station id. number	RGS10
Number of coordinates	4
Geographic coordinates	
Point 1	Latitude: 44,82939911^{O}
	Longitude: 20,41040039^{O}
Point 2	Latitude: 44,82939911^{O}
	Longitude: 20,47769928^{O}
Point 3	Latitude: 44,78290176^{O}
	Longitude: 20,41040039^{O}
Point 4	Latitude: 44,782901762^{O}
	Longitude: 20,47769928^{O}
Number of pixels (column)	35180
Number of pixel (line)	25948
Pixel size *X* axis	0,50 m
Pixel size *Y* axis	0,50 m
DigitalGlobe product level	Basic satellite imagery
Processing level	Standard geometric correction
Image type	PAN
Map projection	Transverse Mercator
Date	WGS84
Image format	GeoTIFF
Image type (bit)	16-bit
Recording time	2011-07-14 09:37 GMT

The image was obtained through the observation of Earth's surface from space, based on central projection. Although the delivered image had already underwent radiometric and sensor correction, its application in measurement and computation pertaining to geodesy, cartography, construction and other areas that require reliable and accurate measurement is not possible without additional processing and corrections that will remove existing deformations.

2.2 Worldview-1 satellite image pre-processing

There are several methods of digital image pre-processing, which produce a new image that is more suitable for use in almost any filed. These procedures are divided into four phases:

– Pre-processing
– Image Quality Improvement
– Image Transformation, and
– Image Classification and Analysis.

Since the delivered image had already been treated for radiometric deformations, the pre-processing procedure carried out in this experiment entailed Image Quality Improvement phase only, which still facilitated subsequent visual analysis and interpretation i.e. significant improvement was achieved in relation to the conspicuity of objects, parts of the image or entire image surface.

Standard computer operations commonly used for the improvement of overall image display were also carried out, observing the original pixel values and keeping their proportional relations. Optimization of the amount of illumination ("Brightness") and emphasizing the pixel difference ("Contrast") were some of the standard computer operations carried out on the subject image.

Improving the contrast and clarity of the image is the most common form of the improvement of the visual appearance of image, which was, in this experiment, achieved by histogram stretching (Fig. 2), that is by rejecting the pixels with greyscale boundary values, taking into consideration only those values that represent the electromagnetic reflection of the image object and expanding the number of the existing levels.

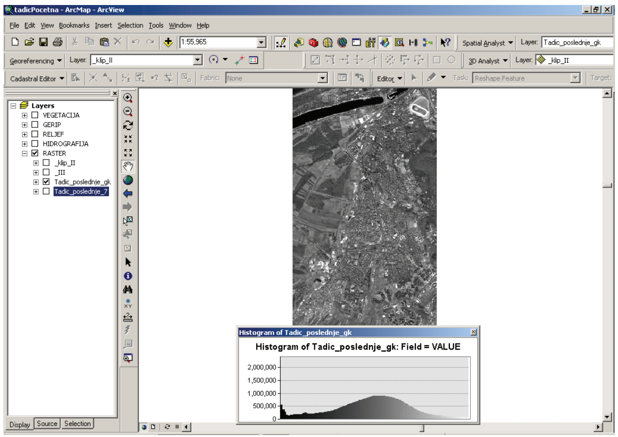

Figure 2 WorldView-1 imagery with histogram

2.3 Orthorectification and georeferencing of the Worldview-1 satellite image of the tested area

Full transformation of an image from central to orthogonal projection is called orthorectification or internal geometric correction. Each pixel of the image corresponds to one point on the ground. In order to eliminate errors that arise as a consequence of the effects of central projection, tilt of the camera axis and terrain relief, imagery must undergo digital orthorectification [8, 9, 10, 1]. Fig. 2 points to a conclusion that corrections are proportional to the distance of a given point on terrain from the image centre and height difference. Original raw image is correlated with the reference geocoded layer which contains information on the height of terrain points. Classic topographic maps (TM), selected control points on the ground surface, or digital elevation terrain model can be used as these bases. In accordance with the information on terrain heights for a given stereo model, spatial curvature and position and size of the relief elements are adjusted, producing an orthoimage of satisfactory accuracy for the given scale. Today, computer orthorectification is the principal method for the production of graphic layers from satellite imagery (Fig. 3). Images corrected in this way are referred to as corrected orthoimages.

In order for the transformation from pixel coordinates to 3D coordinates to be precisely defined mathematical models of sensors are created, combining all the physical elements of the image (the actual model). However, as these models are generally very long and complex mathematical expressions, and each sensor type has a different actual model, a general model was introduced as a polynomial of rational functions (Rational Function Model - RFM), which approximates the physical sensor model and can support the timely calculation and ensure the necessary accuracy.

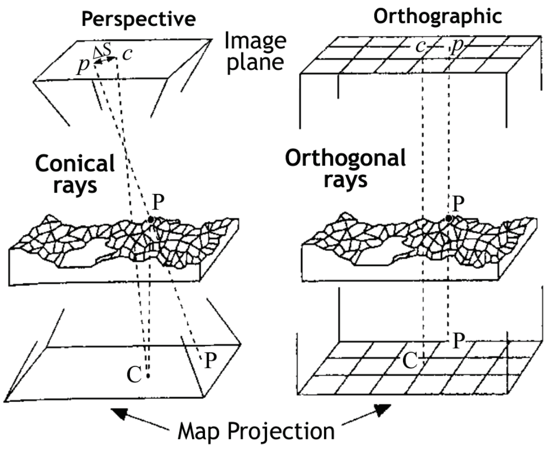

Figure 3 Principle of orthorectification [1]

There are two ways to define the actual sensor model. The main difference between these two methods is whether they use ground control points (GCP). Without the GCP, orientation parameters are derived from satellite ephemerides and altitude. Satellite ephemerides are determined using a GPS receiver mounted on the satellite and a corresponding processing of GPS data on Earth. Satellite altitudes are determined through optimal combination gyro-stellar measurements. Using the GCP highly improves the modelling accuracy.

2.3.1 RFM based orthorectification

The process of orthorectification of satellite images requires the following input data:

- RFM obtained with the image
- Digital Terrain Model (DTM)
- GCP determined through GPS measurements.

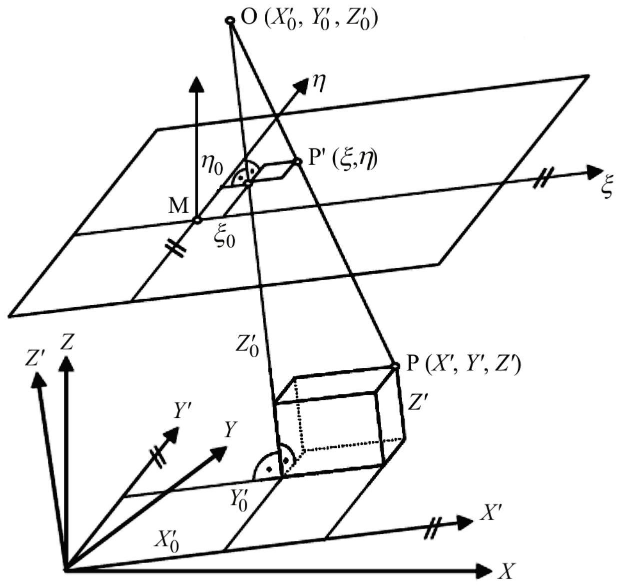

Figure 4 The relationship between object image coordinates (ξ, η) and 3D object coordinates at the time of recording [12]

Rational function model allows us to define the relation between image coordinates (ξ, η) and 3D object coordinates (X, Y, Z) (Fig. 4), that is, in the rational function model pixel coordinates represent the relation between terrain coordinates in a polynomial, which correspond to the latitude, longitude, and height. In an effort to prove the stability of operations, pixel and field coordinates are set in the range from −1 to 1 [11, 12, 7, 8].

For the transformation from terrain to pixel coordinates, relationship defined by a polynomial has a general formula:

$$\xi_n = \frac{P_a(X_n, Y_n, Z_n)}{P_b(X_n, Y_n, Z_n)}, \quad (1)$$

$$\eta_n = \frac{P_c(X_n, Y_n, Z_n)}{P_d(X_n, Y_n, Z_n)}, \quad (2)$$

where ξ_n, η_n represent normalized pixel coordinates, and (X_n, Y_n, Z_n) coordinates denote normalized coordinates of the Earth surface.

To calculate the normalized coordinates the following formulas are used:

$$\xi_n = \frac{\xi - \xi_0}{\xi_s},\ \eta_n = \frac{\eta - \eta_0}{\eta_s}, \quad (3)$$

$$X_n = \frac{X - X_0}{X_s},\ Y_n = \frac{Y - Y_0}{Y_s},\ Z_n = \frac{Z - Z_0}{Z_s}, \quad (4)$$

ξ_n, η_n and ξ_s, η_s denote values of the slope and the scale of pixel coordinates alternately, and correspondingly the X_0, Y_0, Z_0 and X_s, Y_s, Z_s values represent slope values and scale of the coordinates of the object on the ground.

In the Eq. (1) P_a, P_b, P_c, P_d usually denote maximum degrees of a polynomial equation, for 20 corresponding coefficients that can be represented by Eqs. (3) or (4):

$$P_a(X,Y,Z) = a_0 + a_1X + a_2Y + a_3Z + a_4X^2 + a_5XY + \\ + \ldots + a_{17}Y^2Z + a_{18}YZ^2 + a_{18}Z^3, \quad (5)$$

$$P_a(X,Y,Z)=\sum_{i=0}^{m_1}\sum_{j=0}^{m_2}\sum_{k=0}^{m_3}a_{ijk}X^iY^jZ^k, \quad (6)$$

$$0\le m_1\le 3;\ 0\le m_2\le 3;\ 0\le m_3\le 3; \quad m_1+m_2+m_3\le 3. \quad (7)$$

In the RFM coefficients of the first order can represent a deformation of optical projection, while corrections such as the Earth's curvature, atmospheric refraction, and the deformation of optical lens, can be modelled by second order coefficients. Other unknowns or more complex deformations with components of higher order can be absorbed by coefficients of the third order.

In order to precisely define the transformation from pixel coordinates to 3D coordinates, the raw image is correlated with the geocoded reference surface, which contains information on the height of terrain points. These basics can be classic TMs, selected control points of the ground surface, or a digital terrain model.

2.3.2 Digital terrain model (DTM)

Digital Terrain Model – DTM is a simple statistical representation of the continuous land surface by a large number of selected points with known *X*, *Y*, and *Z* coordinates in an arbitrary coordinate field [13].

Generally, DTM can be divided into two basic types:

- DTM based on data arranged in a regular grid of points (GRID), and
- DTM based on a network of irregular triangles, i.e. TIN system (Triangulated Irregular Network).

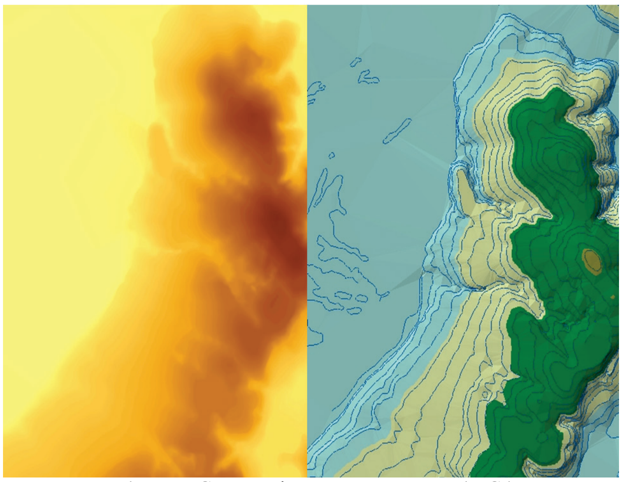

Figure 5 GRID and TIN DTM test area (MGI)

For the orthorectification of the satellite image test area we used a DTM that was generated from a digital elevation model developed in the MGI (Military Geographical institute – Belgrade), through vectorization of contour lines from the scanned TM25. The DTM grid size used in this experiment is 3,0 m, and the average error ($RMSE_{DTM}$) is determined by empirical measurements and is 7 meters (Fig. 5).

For the purpose of determining orientation points, a preliminary analysis of the image was carried out in order to identify the characteristic and easily discernible shapes (shafts, ventilation openings, curbs, etc.) and their distribution in space. In the portion of space that is densely populated and covered with a variety of objects, we have identified a number of details whose coordinates, determined through field measuring, provided a sufficient number of orientation points.

The problem of selecting orientation points in the far western and eastern parts of the image area (uninhabited area with large irregularly-shaped agricultural land and Kosutnjak forest), was mainly solved by determining the orientation points of field paths section and surrounding the forest with a large number of points in order to obtain the best results (Fig. 6).

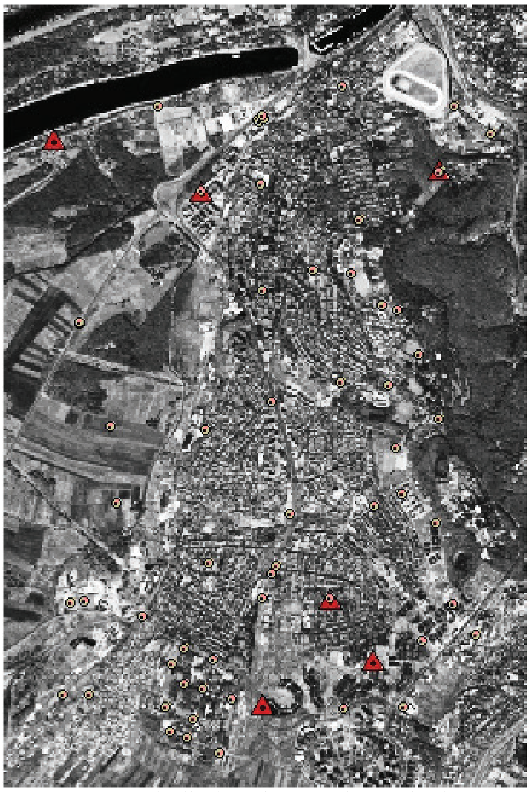

Figure 6 Distribution of GCP and control points

Coordinates of orientation points were determined by field measuring using a Trimble GPS receiver, applying the rapid static positioning method (fast static). All points had positional error below 4,0 cm except one with a 20,0 cm error. Orthorectification was performed using PCI Geomatica software package with rectified RPCs (Rational Polynomial Coefficient), which were determined by the software based on control points and existing RPCs (Basic data on satellite image contains RPCs – Rational Polynomial Coefficients). As stated in the theory, this procedure of coefficient rectification significantly improves the orthorectification accuracy [11].

Based on the known data for the WorldView-1 image (Tab. 1) (CE90raw image error =15,0 m, elevation angle, *E* = 73°05'33", 72), and data on the mean error for DTM (RMSEDTM = 7 m), it can be calculated:

Linear error DTM (error with 90 % probability):

$$LE90_{\mathrm{DMT\_er}}=1{,}654\cdot RMSE_{\mathrm{DMT}}=11{,}58\ \mathrm{m}. \quad (8)$$

DTM error:

$$CE90_{\text{DMT\_er}} = \frac{LE90}{\tan(E)} = 3{,}52\ \text{m}. \quad (9)$$

Orthophoto error:

$$CE90_{\text{orthophoto}} = \sqrt{CE90^2_{\text{DMT\_error}} + CE90^2_{\text{raw\_image\_er}}}, \quad (10)$$

$$CE90_{\text{orthophoto}} = \sqrt{3{,}52^2 + 15^2} = 15{,}41\ \text{m}, \quad (11)$$

$$RMSE_{\text{orthophoto}} = \frac{CE90_{\text{orthophoto}}}{2{,}146} = 7{,}18\ \text{m}. \quad (12)$$

Taking into account the characteristics of the human eye and the nature of digital image it can be assumed that the maximum accuracy of measurement of coordinates is equal to one half of the pixel size $\delta/2$ (where δ denotes the size of one pixel). Errors are assumed to have been independent and equally shared, and the density-voltage function can be represented by the formula:

$$f(\zeta) = \frac{1}{\delta}, \left(-\frac{\delta}{2} < \zeta < \frac{\delta}{2}\right). \quad (13)$$

The root-mean-square error of coordinate measurement:

$$m^2 = \int_{-\sigma/2}^{\delta/2} \zeta^2 f(\zeta) \mathrm{d}\zeta = \frac{\delta}{12}, \quad (14)$$

$$m = \pm 0{,}14\delta,$$

where m denotes the accuracy of manually measured pixel coordinates of a point.

Image error after RPC improvement can be calculated on the basis of the formula

$$RMSE_{\text{image}} = \sqrt{mx^2 + my^2}, \quad (15)$$

where mx and my denote root-mean-square error coordinate roundup on the satellite image.

Since orthorectification was carried out on the basis of repaired RPCs, the accuracy of orthorectified image is calculated using the formula:

$$CE90_{\text{ort.}} = \sqrt{\left(\frac{1{,}654 \cdot RMSE_{\text{DMT}}}{\tan(E)}\right)^2} + \sqrt{(2{,}146 \cdot RMSE_{\text{im.}})^2}. \quad (16)$$

$$CE90_{\text{orthophoto}} = \sqrt{3{,}52^2 + 0{,}880^2} = 3{,}63\ \text{m}. \quad (17)$$

$$RMSE_{\text{orthophoto}} = \frac{CE90_{\text{orthophoto}}}{2{,}146} = 1{,}69\ \text{m}. \quad (18)$$

Repaired RPCs were calculated automatically in the PCI Geomatica software. Reports on errors and orthorectification accuracy evaluation are given in Tables 2 and 3.

Table 2 Report on orthorectification error tolerances

Report on error tolerances				
Data for one image	GCP points:	14	*X* RMS	0,36 m
			Y RMS	0,36 m
	Control points:	18	*X* RMS	0,28 m
			Y RMS	0,34 m

As the error report shows, positioning errors of control points are less than one meter, while in the majority of control points they correspond to the pixel size of half a meter, or are even much lower.

Based on the results given in column 2 of Tab. 3, and the formula for calculating the mean-square-error, it is possible to calculate the error of orthorectification carried out using repaired RPCs.

$$m_x^2 = m_\Delta^2 = \frac{1}{n-1} \cdot \sum \left(X_i - \overline{X}\right)^2, \quad (19)$$

$$RMSE = 0{,}50\ \text{m}. \quad (20)$$

In the previous assessment the obtained mean-square-error of the orthorectified image for calculated RPC coefficients was significantly higher (1,69 m). The experiment showed that the possible positioning accuracy of image points can be significantly less than the pixel size.

2.3.3 Worldview-1 satellite image georeferencing

Satellite image georeferencing entails application of corrections that bring the image into the appropriate map projection and connects it with the national coordinate system. This process is also referred to as external geometric transformations. Georeferencing process involves the following main stages:

- Determining orientation points (arranged as evenly as possible on the entire image)
- Determining screen coordinates of all selected orientation points, and
- Transformation of all pixels of the input image to the output image.

Georeferencing was performed in the PCI Geomatica software package using second degree polynomial. Cubic convolution was chosen for the simultaneous raster recomposition. Georeferencing by polynomial method employed 14 points, while the remaining 18 were used for georeferencing control. RMS (Root Mean Square) stood at 0,26 meters.

Given that all TMs for the territory of the Republic of Serbia were created in the Gauss-Kruger's projection, the next step involved the transformation of the already completed orthophoto maps from the UTM projection. Raster transformation was performed using the ArcGIS 9.3 software package. Transformation parameters (provided in Tab. 4) were obtained from GPS measurements on orientation points that belong to the national trigonometric network.

Table 3 Levelled values of orientation points' coordinates obtained from the orthorectified image

Point ID	Res	Res *X*	Res *Y*	Type	Ground *X*	Ground *Y*	Ground *Z*	Comp *X*	Comp *Y*
35	1,078	−0,151	−1,067	Check	453070,883	4955728,448	104,47	453070,73	4955727,38
45	0,882	0,724	−0,504	GCP	455182,812	4954139,432	91,21	455183,54	4954138,93
37-1	0,820	−0,515	0,637	GCP	452017,028	4955416,212	71,93	452016,51	4955416,85
50	0,670	−0,625	−0,243	GCP	452803,868	4954000,953	135,25	452803,24	4954000,71
27	0,645	−0,606	0,222	Check	454341,864	4956160,098	170,82	454341,26	4956160,32
17	0,629	0,313	−0,545	GCP	454679,446	4957328,378	196,10	454679,76	4957327,83
44	0,606	−0,188	0,576	GCP	454564,593	4954614,693	182,65	454564,40	4954615,27
25	0,528	−0,430	−0,307	Check	452361,596	4956186,558	71,62	452361,17	4956186,25
40	0,512	−0,419	−0,294	Check	452746,974	4954617,400	125,42	452746,55	4954617,11
16	0,447	0,263	−0,361	Check	454400,780	4957704,422	199,90	454401,04	4957704,06
9	0,424	0,424	−0,003	GCP	454162,154	4957944,450	189,02	454162,58	4957944,45
32	0,409	−0,311	−0,264	Check	454708,771	4955124,228	185,37	454708,46	4955123,96
43	0,407	−0,083	0,399	Check	454333,553	4954973,169	181,10	454333,47	4954973,57
18	0,367	−0,164	0,328	Check	454836,379	4956824,546	191,56	454836,21	4956824,87
39	0,360	0,297	−0,203	GCP	452790,965	4954952,287	118,90	452791,26	4954952,08
14	0,358	0,286	−0,214	Check	453487,744	4957817,534	107,30	453488,03	4957817,32
31	0,348	0,108	−0,331	GCP	455119,979	4955166,836	194,30	455120,09	4955166,51
20	0,335	−0,332	−0,047	Check	454444,840	4957091,073	169,03	454444,51	4957091,03
21	0,290	0,213	0,197	Check	454078,640	4957107,052	147,05	454078,85	4957107,25
12	0,282	0,204	0,196	GCP	453008,801	4958569,849	76,49	453009,00	4958570,04
42	0,267	0,254	−0,085	Check	454100,946	4954608,007	176,84	454101,20	4954607,92
1	0,254	0,088	0,238	GCP	451880,109	4958966,566	75,48	451880,20	4958966,80
29	0,220	−0,200	−0,092	Check	454814,691	4956029,590	193,00	454814,49	4956029,50
23	0,189	0,183	0,048	Check	453052,593	4956744,263	94,44	453052,78	4956744,31
24	0,181	−0,031	0,178	GCP	452321,934	4956775,106	71,11	452321,90	4956775,28
41	0,165	0,008	0,164	Check	453487,941	4954634,953	157,36	453487,95	4954635,12
28	0,146	0,129	0,067	GCP	454550,559	4956257,982	190,41	454550,69	4956258,05
8	0,143	−0,135	−0,048	Check	454227,942	4958354,949	169,37	454227,81	4958354,90
33	0,100	0,039	−0,092	GCP	454005,573	4955437,991	169,09	454005,61	4955437,90
15	0,075	−0,043	0,062	Check	454514,863	4957664,872	202,23	454514,82	4957664,93
38-1	0,071	−0,040	−0,059	Check	452567,516	4955317,530	84,92	452567,48	4955317,47
7-1	0,016	0,010	0,013	GCP	454835,410	4958740,157	115,93	454835,42	4958740,17

Table 4 Parameters of transformation from UTM to Gauss-Kruger's projection

Method	7- parameter
Rotation about *X* axis	−0°00'05,14321"
Rotation about *Y* axis	0°00'00,07342"
Rotation about *Z* axis	0°00'13,81196"
Translation along *X* axis	−560,286 m
Translation along *Y* axis	−188,913 m
Translation along *Z* axis	−415,443 m
Scale factor (ppm)	−6,0995

Transformation parameters were calculated using the Trimble Geomatics Office software package.

3 Conclusion

Major satellite missions and programs can successfully meet surveying and construction needs, as the most demanding fields in terms of spatial accuracy. The quality of satellite imagery with a spatial resolution of 1 m to 0,4 m, are the same as or better than the scanned aerial images with a spatial pixel size of 0,6 m, where the required pixel size is determined by the size of the smallest detail on the ground that must be unambiguously spatially defined (power lines, monuments, natural gas pipelines, etc.)

Since the WorldView-1 satellite image is based on the central projection, in order for it to obtain measurement values, the pixels had to be translated from the central to orthogonal projection, due to which it was necessary to carry out the orthorectification process. Using the RPCs obtained along with the image, in the form of text files, and with the help of DTM and additional GCPs, RPCs were rectified and the full orthorectification process greatly improved image position accuracy.

Based on the obtained results it can be concluded that the application in the surveying and construction fields, provided automatic classification of content is not implemented, requires only a simple radiometric image with 8 bit resolution. WorldView-1 image with spatial resolution of 0,5 m can be fully used for the production of geodetic survey maps of 1:10 000 scale and finer. It is possible to carry out content update on maps of 1: 5000 scale. In most cases, bearing in mind what has already been said, rectification of images of high spatial resolution such as the WorldView-1 image, it is sufficient to have a DTM (Digital Model of Terrain), generated from a digital elevation model by vectorization of contour lines of a scanned topographic map in a scale of 1:25 000, grid size 3 m, with a mean error (RMSEDTM) 7 meters.

Given the progress of satellite missions and technology of sensor production, that is, higher resolution of source spatial image, it can be assumed that in the foreseeable future satellite images will gain dominance over conventional aerial images. However, this anticipated transfer from aerial photogrammetric images to satellite images may be delayed by the advent of digital multispectral aerial cameras with sensors of similar quality to those of satellite sensors.

Acknowledgements

The work reported in this paper is a part of the investigation within the research project TR 36017 supported by the Ministry for Science and Technology, Republic of Serbia. This support is gratefully acknowledged.

4 References

[1] Jensen R. J. Remote sensing of the environment – an earth resource perspective, Second edition, University of South Carolina, USA, 2007.
[2] Lutz, A. D.; Washington-Allen, A. R.; Shugart, H. H. Remote sensing of boreal forest biophysical and inventory parameters. // Canadian Journal of Remote Sensing. 34, 2(2008), pp. 286-313.
[3] Seletković, A.; Pernar, R.; Ančić, M.; Sučić, J. Assessment of Stand Structural Elements on the Basis of Spectral Reflectance Values of an IKONOS Satellite Image. // Croatian Journal of Forest Engineering, University of Zagreb, Croatia, 32, 1(2011), pp. 329-343.
[4] Baltsavias, E. P.; Pateraki, M.; Zhang, L. Radiometric and geometric evaluation of IKONOS geo images and their use for 3D building modelling. Joint ISPRS Workshop on "High Resolution Mapping from Space 2001", Hannover, Germany, 19-21 September 2001.
[5] Tadić, V.; Sekulović, D.; Tatomirović, S. Cartographic analysis of urban areas using satellite image as a base for data collecting. // Bulletin of the Serbian geographical society. XC, 3 (2010), pp. 225-237.
[6] Deilami, K.; Hashim, M. Very High Resolution Optical Satellites for DEM Generation. // A Review, European Journal of Scientific Research. 49, 4 (2011), pp. 542-554.
[7] Toutin, T. Review article - Geometric processing of remote sensing images: models, algorithms and methods. // International Journal of Remote Sensing. 10, (2004), pp. 1893-1924.
URL: http://dx.doi.org/10.1080/0143116031000101611 (12. 2. 2013).
[8] Fraser, C. S.; Hanley H. B. Bias compensation in rational functions for Ikonos satellite imagery. // Photogrammetric Engineering and Remote Sensing. 69, 1(2003), pp. 53-57.
[9] Capaldo, P.; Crespi, M.; Fratarcangeli, F.; Nascetti, A.; Pieralice, F. DSM generation from high resolution imagery: applications with WorldView-1 and Geoeye-1. // Italian Journal of Remote Sensing. 44, 1(2012), pp. 41-53.
[10] Fraser S. C.; Hanley B. H. Bias-compensated RPCs for Sensor Orientation of High-resolution Satellite Imagery. // Photogrammetric Engineering & Remote Sensing. 71, 8(2005), pp. 909-915.
[11] Jeff Zhizhong Xu. The Rational Function Model (RFM) in Photogrammetric Mapping: Method and Accuracy, Department of Earth and Space Science & Engineering, York University, 2004.
[12] Kraus, K. Fotogrametrija, Naučna knjiga, Beograd, 1987. (translated by Dušan Joksić).
[13] Petrie, G.; Kennie, T. J. M. Terrain Modelling in Surveying and Civil Engineering. Whittles, London, 1990.

Authors' addresses

dr Goran Ćirović, professor
The Belgrade University College of Civil Engineering and Geodesy
Belgrade, Serbia
E-mail: cirovic@sezampro.rs

dr Miodrag Regodić, associate professor
Ministry of Defence of the Republic of Serbia
University of Defence in Belgrade, Serbia
E-mail: mregodic62@gmail.com

dr Dragoljub Sekulović, associate professor
Ministry of Defence of the Republic of Serbia
University of Defence in Belgrade, Serbia
E-mail: sekulovicdr@yahoo.co.uk

mr Vladan Tadić, assistant
Ministry of Defence of the Republic of Serbia
Belgrade, Serbia
E-mail: tadicvladan@yahoo.com

dr Ljubomir Gigović, assistant professor
Ministry of Defence of the Republic of Serbia
University of Defence in Belgrade, Serbia
E-mail: ljgigovic@yahoo.com